ISSN NO. 2320-5407

Journal homepage: http://www.journalijar.com

INTERNATIONAL JOURNAL OF ADVANCED RESEARCH

RESEARCH ARTICLE

Synthesis, crystal structure, spectral characterization, antiproliferative / DNA interaction studies of monomeric ruthenium (II) manganese (II) and palladium (II) complexes of a novel 2-benzoylhydrazine carbothioamide

M. Umadevi[1], V. Muthuraj[2] and P. Saravana Bhava[3]

1. PG & Research Department of Chemistry, Nehru Memorial College, Puthanampatti, Tiruchirappalli, Tamilnadu, India.

2. PG & Research Department of Chemistry, V.H.N.S.N.College, Virudhunagar,Tamilnadu, India.

3. Department of Chemistry, S.Vellaichamy Nadar Polytechinc College, Virudhunagar, Tamilnadu, India.

Manuscript Info

Manuscript History:

Received: 15 June 2013
Final Accepted: 25 June 2013
Published Online: July 2013

Key words:
Thiosemicarbazone,
Cytotoxicity,
Crystal structure,
DNA binding,
Oxidative cleavage.

Abstract

A novel 2-benzoylhydrazinecarbothioamide (bhct) ($C_8H_9N_3OS$) and its transition metal complexes $[Pd(C_8H_9N_3OS)_2]$, $[Ru(C_8H_9N_3OCl_2S)_2]$, $[Mn(C_8H_9N_3OCl_2S)_2]$ have been synthesised and characterized by elemental analysis, IR, UV, MS, NMR and single-crystal X-ray diffraction studies. Molecular structure of the ligand is established by single crystal X-ray structural analysis. A distorted octahedral structure is assigned 2:1 Mn(II) and Ru(II) complexes while the Pd(II) complex has tetragonally distorted square planar geometry. In all three complexes, the ligand acts as bidentate with N, S donor sites. The complexes and their synthetic precursor are tested for *in vitro* antitumor activity on human breast cancer MCF-7 cell lines. The Ru (II) complex is an avid DNA binder with a binding constant $2.3 \pm 0.4 \times 10^4$ M^{-1}. Observed changes in the UV, Emission and viscosity of CT-DNA solution in the presence of Ru(II) complex, suggests electrostatic binding.

Copy Right, IJAR, 2013,. All rights reserved.

Introduction

Coordination chemistry of mixed hard-soft N, S donor ligands is a field of current interest. The important factor is the design of ligands with an appropriate structural backbone, thiosemicarbazones. The most widely studied are sulfur and nitrogen consisting ligands [1]. They also stabilize uncommon oxidation states and generate a different coordination number in transition metal complexes in order to participate in various redox reactions [2]. The chemistry of transition metal complexes of thiosemicarbazones has received considerable attention for their bioinorganic relevance [3] such as antibacterial, antimalarial, antiviral and anti tumor activities [4, 5]. It is well known that several metal ions enhance and modify the biological activities of thiosemicarbazones. Much attention has been drawn towards the chemistry of Ru [6] and Rh [7] in different coordination spheres but very little work has been reported on Pd(II) complexes with substituted thiosemicarbazone ligands.

Medicinal inorganic chemistry exploits the unique properties of metal ions for the design of new drugs. For instance, the clinical application of chemotherapeutic agents for cancer treatment, such as cisplatin. The use of cisplatin is, however, severely limited by its toxic side effects. This has spurred chemists to employ different strategies in the development of new metal-based anticancer agents with different mechanisms of action. Apoptosis is a biological phenomena that involves in process ranging from embryogenesis to ageing, from normal tissue homoeostasis to many human diseases. Apoptotic cells share a number of common features such as cell shrinkage, nuclear condensation, membrane blabbing, chromatin cleavage, and formation of pyknotic bodies of condensed chromatin. The anti-proliferative properties of the chemical compounds are predetermined using MTT assay.

As part of continuous research on Ru(II) and Pd(II)complexes of 2-enzoylhydrazineCarbothioamide ligand, the aim is to

exploit the versatility of coordination behaviour of Ru(II), Pd(II) and Mn(II) complexes with ligand. A four coordinated Pd(II) and six coordinated Ru(II) and Mn(II)complexes of 2-benzoylhydrazinecarbothioamide are obtained. In this paper, the synthesis, spectroscopic characterization, crystal structure and cytotoxicity studies of both ligands and complexes are repoted.

2. Experimental

2.1. Materials and Instrumentation

Benzoylchloride, thiosemicarbazone and metal halide salts are purchased from E-Merck and used without further purification. Ethanol refers to absolute ethanol unless otherwise specified. Solvents are obtained from commercial sources and used as received. Nuclear magnetic resonance spectroscopic measurements are made on Bruker 300 MHz spectrometer (0-15δ). Deuterated organic solvents along with tetramethylsilane (TMS) as the internal standard is used. Infrared spectra for all the complexes and ligands are recorded on a JASCO FT-IR–410 (4000-400 cm^{-1}) spectrophotometer. Potassium bromide disc is employed for sample preparation. The instrument was calibrated against polystyrene film. Electronic absorption spectral measurements were recorded in solution using JASCO V-550 UV-Vis spectrophotometer, and diode array spectrophotometer (Analytica Jena specord S 100).

The data for single crystal X-ray studies are collected with Mo-kα radiation at 293˚K on CAD-4 Express [8]; cell refinement; CAD-4 Express device. A semi empirical correction is applied using XCAD4 [9]. The structures are solved by direct methods using SHELXTL/PC; (molecular graphics) and completed by iterative cycles ΔF syntheses, using the SHELXTL/PC package.

2.2. Synthesis of 2-benzoylhydrazine carbothioamide

The compound is prepared in high yield from a reaction of thiosemicarbazone (0.272 g/ 20 M) in aqueous ethanol (1:1) and benzoylchloride (0.172 g/ 20 M) in ethanol and the reaction mixture is allowed to stir for 2 hrs. The colourless product is separated, filtered, washed with hot ethanol and recrystallised from aqueous ethanol. The product is dried in vacuo over fused calcium chloride and stored in a desiccator. Single crystals are obtained by slow evaporation of solution of compound in water-ethanol (2:1) mixture (**Scheme 1**). Anal. (Calc) found for [$C_8H_9N_3OS$; C, (49.32), 49.73; H, (4.72), 4.92; N, (21.63), 21.78); $Pd(bhct)_2$; $C_{16}H_{18}N_6O_2S_2Pd$; C, (38.57), 38.76; H, (3.56), 3.73; N, (16.94), 17.09; Ω ($ohm^{-1}cm^{-1}M^{-1}$): 142 $Mn(bhct)_2$; $C_{16}H_{18}N_6O_2Cl_2S_2Mn$; C, (37.24), 37.68; H, (3.46), 3.81; N, (16.35), 16.65; Ω ($ohm^{-1}cm^{-1}M^{-1}$): 146 $Ru(bhct)_2$; $C_{16}H_{18}N_6O_2Cl_2S_2Ru$; C, (34.23), 34.81; H, (3.23), 3.63; N, (14.85), 15.10; Ω ($ohm^{-1}cm^{-1}M^{-1}$): 138].

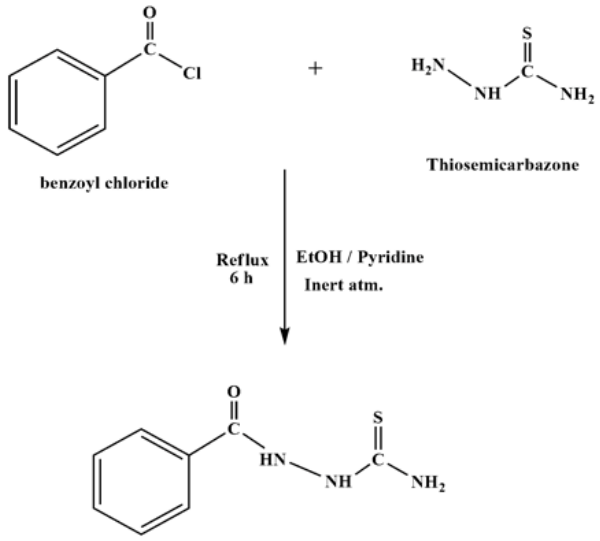

Scheme.1. Synthesis of 2-benzoylhydrazine carbothioamide

2.3. Synthesis of Ru(II) & Mn(II) complexes

20 ml of methanolic solution of $RuCl_3.5H_2O$ (0.26 g / 1 M) / $MnCl_2.4H_2O$ (0.198 g/ 1M) is added slowly to a magnetically stirred 15ml methanolic solution of the ligand (0.46 g / 2M). The mixture is stirred under nitrogen atmosphere with the addition of triethylamine (0.05 ml, 0.36 mmol) until a deep brown color solution is formed. After that 10 ml aq.KOH (0.5 g, 0.89 mmol) is added and the mixture is refluxed for 12 hrs. The solution is kept to cool at room temperature. The solid complex is separated, washed with water and dried in vacuum over CaO (**Scheme 2**).

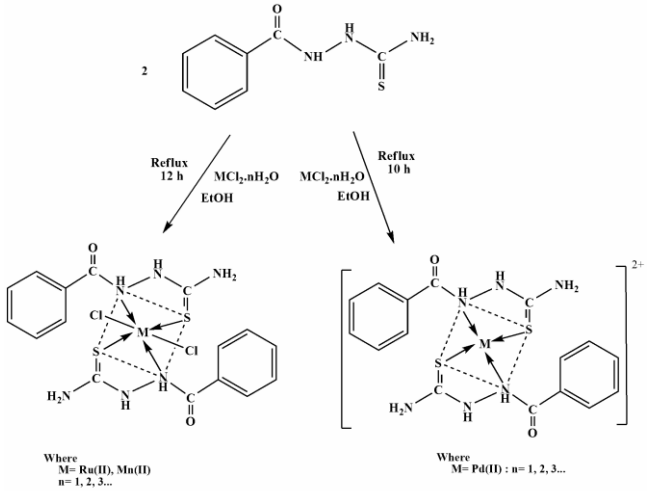

Scheme. 2. Synthesis of Ru(II) & Mn(II)complexes

2.4. Synthesis of Pd(II) complexes

Palladium(II) complexes are prepared by mixing 0.177 g / 1mmol of $PdCl_2.4H_2O$ in ethanol, few drops of HCl with the solution of ligand (0.46 g /2 mmol) by dissolving in hot aqueous ethanol / $CHCl_3$ (1:1) solution. The reaction mixture is refluxed at 70˚C for 10 hrs and the pH of the solution is adjusted to 7 by adding few drops of liq.NH_3, after that the solution is kept at room temperature. Colored palladium(II) complex thus separated is filtered, washed successively with cold ethanol to remove unreacted ligands and then air dried.

2.5. Cell culture

The breast cancer cell line MCF-7 is provided by Dr. B. Kadalmani (Wadsworth Center, Albany, NY, USA). The cells were grown in RPMI-1640 medium supplemented with 20% fetal bovine serum (FBS), 50 **l**g/ml streptomycin, 50 U/ml penicillin G, and 2 mM L-glutamine.

MTT, (3-(4, 5-Dimethyl thiazol-2yl)-2, 5-diphenyl tetrazolium bromide), is cleaved by mitochondrial dehydrogenase of viable cells, yielding a measurable purple formazan product. This formazan production is proportionate to the viable cell number and inversely proportional to the degree of cytotoxicity [10].

2.6. DNA binding and cleavage

All experiments involving interaction of DNA are carried out in Tris buffer (pH 7.1). A solution of calf thymus DNA in the buffer gives the ratio of UV absorbance at 260 and 280 nm of about 1.9:1, indicating that the DNA is sufficiently free from protein [11]. The DNA concentration per nucleotide is determined by absorption spectroscopy using the molar absorption coefficient (6600 $M^{-1}cm^{-1}$) at 260 nm [12]. Intense MLCT bands are monitored to follow the interaction of the complex with CT-DNA. Absorption titration experiments are carried out by varying the DNA concentration (0-600 µM) and maintaining the metal complexes concentration constant (5 µM). Absorbance values are recorded after each successive addition of DNA solution.

The gel electrophoresis experiments are performed as described earlier [13]. Supercoiled pUC 19 DNA (500 mg) is treated with 20-100 µM samples of the metal complexes and the mixtures were incubated for 30 min in the dark followed by 1 h irradiation. The reaction is quenched by addition of gel loading dye containing 0.2 M EDTA (EDTA = ethylenediaminetetraacetic acid). The samples are analyzed by electrophoresis for 3 h at 60 V on 1 % agarose gel in Tris-HCl buffer (pH 7.1). The gel is stained with 1 mg/ml ethidium bromide and photographed under UV light.

2.7. Crystallography of bhct ($C_8H_9N_3OS$)

Single crystals are grown up by slow diffusion of aqueous ethanolic solution of the compound. The unit cell dimensions are determined by a least-squares fit of 25 machine-centered reflections ($15.18 < 2\theta < 27.08°$). Data are collected on an Enraf-Nonius CAD-4 diffractometer using graphite-monochromated Mo-kα radiation (i**)** 0.7107 Å) by θ-2θ scans within the angular range 3.0°-45.0°. Three standard reflections measured for every 3600 s of X-ray exposure shows no significant intensity variation over the course of data collection. X-ray data reduction and structure solution and refinement are done using the SHELXTL/PC package. The structure is solved by the Patterson method. Final cycles of refinement converges with discrepancy indices of R= 0.043 and Rw =0.064. A summary of the key crystallographic information is given in Table 1. Further details on the crystal structure investigation is deposited with the Cambridge crystallographic data center as supplementary publication number CCDC 742968 The data can be obtained free of charge via http://www.ccdc.cam.ac.uk/conts/retrieving.html or from e mail: deposit@ccdc.cam.ac.uk.

Table 1. Crystal data and structure refinement for bhct

Identification code	bhct
Formula weight	390.48
Temperature	293(2) K
Wavelength	0.71073 A
Crystal system, space group	triclinic,P-1
Unit cell dimensions	a = 8.2265(3) Å alpha = 83.512(2) deg. b = 8.4224(3) Å beta = 75.568(2) deg c = 14.5692(5) Å gamma = 85.024(2) deg.
Volume	969.54(6) $Å^3$
Z, Calculated density	2, 1.338 Mg/m^3
Absorption coefficient	0.297 mm^{-1}
F(000)	408
Crystal size	0.55 x 0.08 x 0.08 mm
Theta range for data collection	1.45 to 34.06 deg.
Limiting indices	-12<=h<=12, -12<=k<=12, -21<=l<=22
Reflections collected / unique (R_{int})	26506 / 7280 = 0.0252]
Completeness to theta	(υ = 34.06) 91.7%
Refinement method	Full-matrix least-squares on F^2
R_{1obs}, wR_{2obs}	0.0439 / 0.1261
R_{1all} , $wR_{2\ all}$	0.0649 / 0.1529
Extinction coefficient	0.022(4)

3. Results and Discussion

All the complexes (Ru(II), Pd(II) & Mn(II)) are colored, non-hygroscopic solids, stable in air and soluble in DMSO. The elemental analyses show stoichiometry ML_2X_2, where L stands for ligand moiety, X- halide. The molar conductance value indicates the electrolytic nature of the complexes. Both the ligand and Ruthenium (II) complexes are tested for cytotoxicity against a human breast cancer cell lines representative of some important types of human tumors (MCF-7). All compounds exerts concentration-dependent antiproliferative effects after 24 h exposure.

3.1. ^{1}H NMR Spectra

^{1}H NMR spectrum of the ligand, recorded in DMSO-d_6 shows positive signals. The ligand (Fig. 1) has the characteristic resonance of amide nitrogen (CO-NH) proton at 7.89 ppm and the signals are located at 10.49 ppm, 9.25 ppm ascribes to the protons of amine (-N-NH) and thiol (-SH) [14]. The signals of aromatic protons lie in the range of 7.42-7.59 ppm. Because of the non-equivalancy, the NH_2 protons of the ligand appears as doublets at 7.80 -8.50 ppm. This evidence attributes to the restricted rotation around C-N bond (thiocarbonyl carbon and terminal nitrogen) due to its partial double bond character [15]. The presence of the benzoyl group on the terminal amine (NH-C=O-Ph) produces chemical shift at 2.48 ppm, indicates. substitution reaction is carried over benzoyl chloride with thiosemicarbazone.

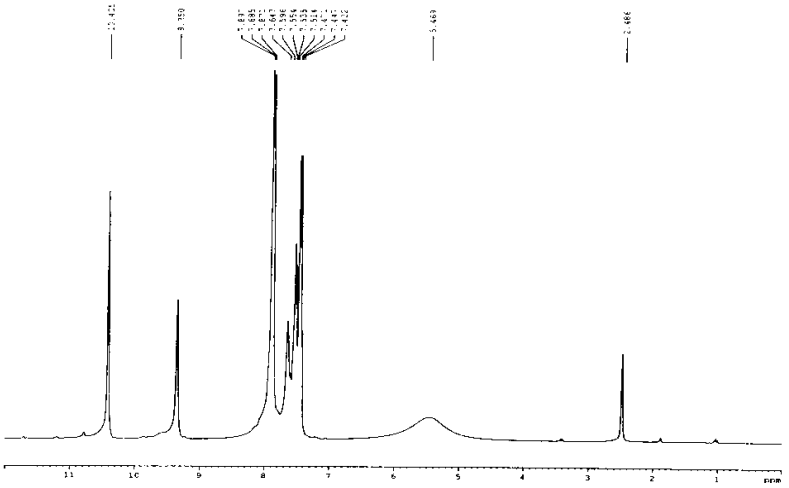

Fig. 1. ^{1}H NMR Spectrum of 2-benzoylhydrazine carbothioamide

3.2. ^{13}C NMR Spectra

The ^{13}C NMR spectrum reveals the presence of expected number of signals corresponding to different types of carbon atoms present in the compound. The spectrum of the ligand exhibits a strong band at 179.2-180.2 ppm and is assigned C=S group. The signals due to amide carbon occurs at 166.3 ppm as downfield peak, while the carbon resonance signals of C=O group appeared at 166 ppm. The C=S signals observed at 178.5-176.6 ppm are characteristic of this group, while the aromatic carbons are observed at δ 139.4-124.5 ppm.

3.3. Molecular Structure Description

A perspective view of the molecular structure of the compounds is illustrated by the ORTEP 36 drawing in Fig. 2. The packing of the molecule is presented in the respective unit cell and is displayed in Fig. 3. The compound crystallizes in the triclinic space group P -1 with Z = 2 (Table 1). Table 2 and Table 3 summarizes the important bond distances and angles as well as some intermolecular O-H contacts. As shown in Fig. 3, in the solid state, the free ligand bhct remains in its thione form (supported by the presence of hydrazinic N−H and C−S distance of 1.7160 (12) Å, which is much shorter than a single C−S bond).

Table 2. Bond lengths [A] for bhct

Bond lengths		Bond lengths		Bond lengths		Bond lengths	
N(1)-C(1)	1.3100(16)	N(2)-H(2)	0.8600	C(11)-C(16)	1.365(3)	C(15)-H(15)	0.9300
N(1)-H(1A)	0.83(2)	C(9)-N(4)	1.3167(18)	C(11)-C(12)	1.382(3)	C(14)-H(14)	0.9300
N(1)-H(1B)	0.851(19)	C(9)-S(2)	1.6846(13)	C(16)-C(15)	1.392(3)	C(8)-C(7)	1.389(2)
N(5)-C(9)	1.3442(17)	N(6)-C(10)	1.358(2)	C(16)-H(16)	0.9300	C(8)-H(8)	0.9300
N(5)-N(6)	1.3827(16)	N(6)-H(6)	0.8600	C(12)-C(13)	1.387(3)	C(4)-C(5)	1.390(3)
N(5)-H(5)	0.8600	C(10)-O(2)	1.211(2)	C(12)-H(12)	0.9300	C(4)-H(4)	0.9300
N(3)-C(2)	1.3241(16)	C(10)-C(11)	1.489(2)	C(3)-C(4)	1.385(2)	C(7)-C(6)	1.369(3)
N(3)-N(2)	1.3847(14)	C(2)-O(1)	1.206(2)	C(3)-C(8)	1.383(2)	C(7)-H(7)	0.9300
N(3)-H(3)	0.8600	C(2)-C(3)	1.4913(18)	C(13)-C(14)	1.348(5)	C(5)-C(6)	1.366(3)
C(1)-N(2)	1.3241(16)	N(4)-H(4A)	0.84(2)	C(13)-H(13)	0.9300	C(5)-H(5)	0.9300
C(1)-S(1)	1.7160(12)	N(4)-H(4B)	0.91(2)	C(15)-C(14)	1.352(5)	C(6)-H(6)	0.9300

Table 3. Bond angles [deg] for bhct

Bond angles		Bond angles		Bond angles	
C(1)-N(1)-H(1B)	117.9(13)	N(4)-C(9)-S(2)	122.73(11)	C(16)-C(11)-C(10)	123.52(17)
H(1A)-N(1)-H(1B)	117.4(18)	N(5)-C(9)-S(2)	119.63(10)	C(12)-C(11)-C(10)	117.00(18)
C(9)-N(5)-N(6)	121.05(12)	C(10)-N(6)-N(5)	120.23(13)	C(11)-C(16)-C(15)	119.5(3)
C(9)-N(5)-H(5)	119.5	C(10)-N(6)-H(6)	119.9	C(14)-C(15)-C(16)	120.9(3)
N(6)-N(5)-H(5)	119.5	N(5)-N(6)-H(6)	119.9	C(14)-C(15)-H(15)	119.6
C(2)-N(3)-N(2)	117.88(11)	O(2)-C(10)-N(6)	121.88(14)	C(16)-C(15)-H(15)	119.6
C(2)-N(3)-H(3)	121.1	O(2)-C(10)-C(11)	122.94(15)	C(15)-C(14)-C(13)	119.8(2)
N(1)-C(1)-N(2)	119.90(11)	N(6)-C(10)-C(11)	115.18(14)	C(15)-C(14)-H(14)	120.1
N(1)-C(1)-S(1)	122.75(10)	O(1)-C(2)-N(3)	121.51(13)	C(13)-C(14)-H(14)	120.1
N(2)-C(1)-S(1)	117.34(9)	O(1)-C(2)-C(3)	123.21(14)	C(7)-C(8)-C(3)	120.44(15)
C(1)-N(2)-N(3)	122.09(11)	C(9)-N(4)-H(4A)	115.2(13)	C(7)-C(8)-H(8)	119.8
C(1)-N(2)-H(2)	119.0	C(9)-N(4)-H(4B)	116.9(12)	C(3)-C(8)-H(8)	119.8
N(3)-N(2)-H(2)	119.0	H(4A)-N(4)-H(4B)	127.3(17)	C(3)-C(4)-C(5)	119.86(19)

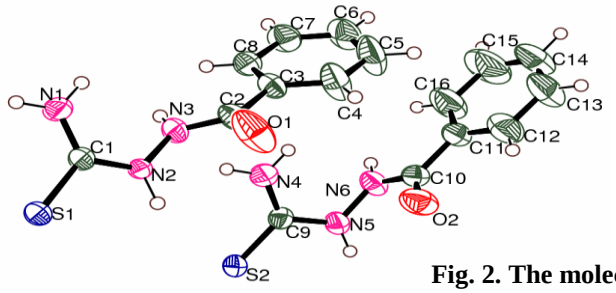

Fig. 2. The molecular structure of 2-benzoylhydrazine carbothioamide

The crystal structure of the ligand has an essentially non-planar conformation which differs markedly form that imposed by coordination. The phenyl ring C8-C13 and the dihedral angles of 120.4 Å and 119.8 Å with the central mean plane through N3-N4-C7 and N5 atom of the thiosemicarbazone residue. Two rotations, one about C4-C5 bond and another about N4-C7 bond by 180° in the metal-free ligand are necessary to achieve the conformation adopted by both ligands in P-1. The molecules of ligand are associated in centro symmetric dimmer via hydrogen bonding interactions of the type N4-H---S, (-X+3, -Y+1, -Z+1) [N4-H + 0.88 A°, H----S1 = 2.691 A°, N4-S1=3.368 A°, N4-H----S1 = 174.08°]. Although it is intermolecular H-bond N5-H---N3 [N5-H = 0.794A°, H---N3 = 2.159A°, N5---N3 = 2.585A°, N5-H---N3 = 113.90°] is also of note.

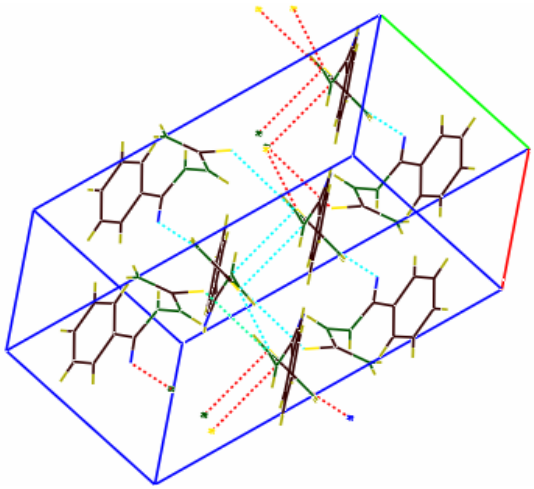

Fig. 3. The packing of the molecule is presented in the respective unit cell

3.4. IR Spectra

The most important bands in the infrared spectra of the ligand (bhct) and its transition metal (II) complexes are presented in Table 4 along with their tentative assignments. The strong bands observed at 3460 cm^{-1} in the free ligand are assigned to υ_{N-H} vibrations. The possibility of thione-thiol tautomerism (H-N-C=S) (C=N-SH) in the ligand is ruled out for no bands around 2700-2500 cm^{-1}, characteristic of thiol group is displayed in the infrared observation.

The spectrum of the ligand shows that it behaves as neutral bidentate and the metal (II) is coordinated through N atom of amide group and S atom of the thioamide group. A broad band observed in the IR spectrum of the free ligand at 3197 cm^{-1} is attributed to the NH moiety linked to the benzoyl group. The other bands observed in the spectrum at ~2922, ~1534, ~1065 and ~1050 cm^{-1} are due to υ(aromatic C-H), υ(C=O), υ(C-N), υ(N-N), and υ(C=S), respectively. The υ(C-N) band of the free ligand at 1632 cm^{-1} is shifted to lower frequency about 20-30 cm^{-1} in the spectrum of complexes. This confirms the coordination of amide nitrogen to the metal atom.

Further, the strong band observed at 879 cm^{-1} is shifted to higher wave number region in all metal complexes. This indicates that thione sulfur participate as a coordinating site. This prediction is confirmed by the presence of new band at ~410 cm^{-1} which can be assigned to υM-S [16]. All the complexes shows a new band around ~474 cm^{-1}, compared with the free ligand and it is assigned to metal-nitrogen stretching vibrations in agreement with the literature data [17].

Table 4. Key IR bands (cm^{-1}) of ligands and their complexes.

Compound	υ_{N-H}	$\upsilon_{C=N}$	$\upsilon_{C=S}$	υ_{N-N}	$\upsilon_{C=O}$	υ_{M-N}	υ_{M-S}
bhct	3460	1632	879	1065	1534	--	--
$(bhct)_2Pd$	3468	1619	919	1070	1537	418	385
$(bhct)_2Mn$	3462	1617	1049	1071	1536	442	394
$(bhct)_2Ru$	3465	1614	1016	1067	1532	474	410

3.5. Electronic spectra

The geometry of the metal complexes has been deduced from electronic spectra and magnetic data of the complexes. Electronic absorption spectrum of bhct and its Ru(II), Pd(II) and Mn(II) complexes are recorded from DMSO solution (10^{-4} M) at room temperature. The electronic absorption spectrum of ligand shows two bands at 260 nm and 288 nm which may be attributed to π- π* and n- π* of >C=O group [18].

Pd(II), Ru(II) complexes are diamagnetic as expected for low-spin. In Ru(II) complex, on the basis of its intensity and position, lowest energy absorption bands in the visible region at ~478 and 427 nm are tentatively assigned to Mdπ→L* metal to ligand charge transfer transitions (MLCT). The bands in high-energy side at ~ 215-290 nm are assigned to intra-ligand π → π*/ n → π* transitions [19]. Coordination of the ligands through both S and N donor sites results to a blue shift in the position of Mdπ→L* transitions. It is attributed to the formation of strained six membered chelate complexes.

The UV-Vis spectrum of Mn(II) complex has maxima at 648 nm, 426 nm, 361 nm and 239 nm, and these bands are assigned to the transitions: $^6A_1 \rightarrow {}^4T_1$, $^6A_1 \rightarrow {}^4E$ / $^4A_1$, $^6A_1 \rightarrow {}^4E$ and $^6A_1 \rightarrow {}^4T_1$. Pd^{2+}, which has d^8 configuration, favors the formation of

complexes with square planar geometry. However, in complexes containing sulfur donors strong charge-transfer transition invariably interferes and prevents observing all the expected bands [20, 21]. In the electronic spectrum of the present Pd^{2+} complex , two spin allowed d-d bands along with two charge transfer bands (220-350 nm) are observed. The charge transfer bands (LMCT) are observed as a combination of $^1A_1g \rightarrow {}^1A_2u$, $^1A_1g \rightarrow a^1Eu$ and $^1A_1g \rightarrow b^1Eu$ transitions respectively. The electronic spectra of these complexes are indicative of planar geometries and the data are in good agreement with previous reports [22]. The absorption spectrum of complex observed with different maxima, in the range 337–483 nm, is assignable to a combination of sulfur→metal(II), nitrogen→metal(II) charge-transfer and M(II) d–d bands [23].

3.6. Mass spectra

For valuable structural information, the complexes of Ru(II), Pd(II) and Mn(II) are investigated by mass spectrometric measurement. Appearance of the peak at 196 amu in free ligand ($C_8H_9N_3OS$) calculated atomic mass 195 amu) corresponds to molecular ion peak and other peaks at 105, 137, 178 & 160 amu due to different fragment steps. The intensity of these peaks gives an idea about the stability of these fragments and their assignments as discussed in scheme 3. For complexes in series $(bhct)_2Pd$, $(bhct)_2Mn$ and $(bhct)_2Ru$ parent peak have been observed at 496, 514 and 560 amu respctively in FAB-MS spectra. The FAB-MS analysis of all compounds exhibited molecular peaks corresponding to compounds with two ligand molecules $[ML_2X_2]$.

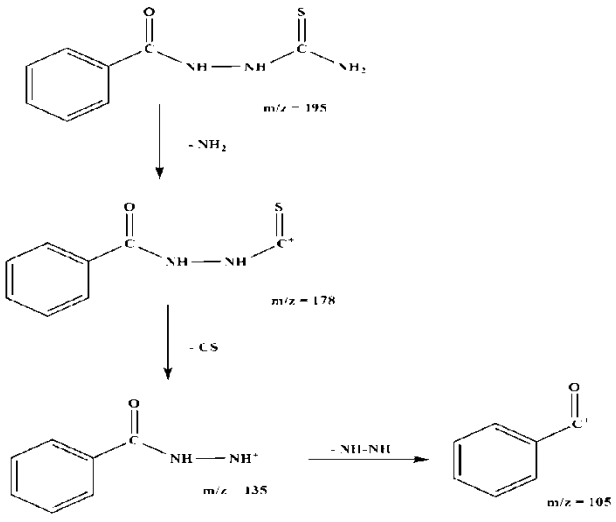

Scheme. 3. Mass fragments of the ligand 2-benzoylhydrazinecarbothioamide

3.7. Biological Studies

3.7.1. DNA binding studies

Electronic absorption spectroscopy a useful experimental technique for probing metal ion-DNA interaction. The UV-Vis spectra of the representative complexes of $(bhct)_2Pd$ and $(bhct)_2Ru$ is monitored in both the presence and absence of CT-DNA. The UV-Vis spectra of these two complexes in acetonitrile are exhibit bands at 285 nm and 370 nm that arises from inter ligand π-π* transition and 449 nm, 450 nm are exhibits metal-ligands charge transfer (MLCT) transition. A fixed concentration (5µM) of the $(bhct)_2Ru$ and $(bhct)_2Pd$ complexes is titrated with increasing concentrations of DNA over a range of 0 - 60 µM, the spectral changes of complexes upon addition of CT-DNA are shown in Fig.4 & Fig.5.

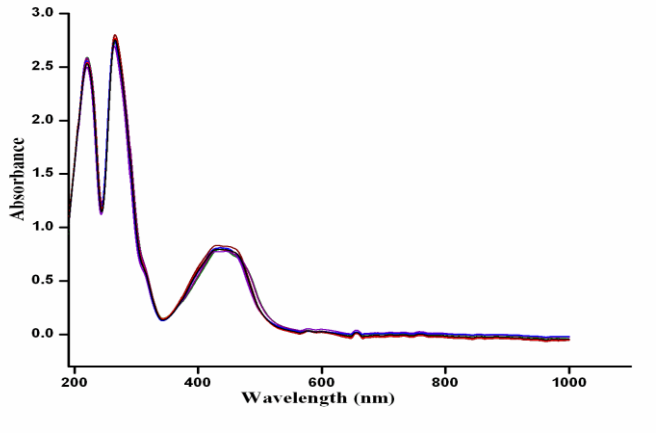

Fig. 4. The UV-Vis spectra of the representative complexes of $(bhct)_2Pd$ and $(bhct)_2Ru$

The peaks shift progressively toward a limit, which represents a spectrum of the complex in a fully complexed form. The addition of CT-DNA resulted in hypochromism for the π-π* absorption at 370 nm compound $(bhct)_2Ru$ and compound $(bhct)_2Pd$ with bathochromic shifts of 9 nm and π-π* absorption at 285 nm with bathochromic shift of < 2 nm and the MLCT absorption of 450 nm with small red shifts of < 2 nm. The small hypchromism and red shifts observed for the ligand-based π-π* absorption at 449 nm are comparable to those observed for typical DNA intercalators.

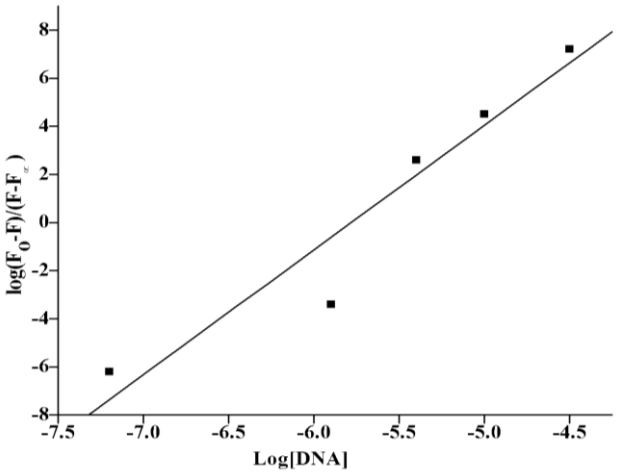

Fig. 5 A plot of [DNA] / ($\varepsilon_a - \varepsilon_f$) Vs [DNA]

A plot of [DNA] / ($\varepsilon_a - \varepsilon_f$) Vs [DNA] gives K_b as the ratio of the slope to intercept and found to be 2.3 ± 0.4 × 10^4 M^{-1} which is lesser than the reported typical intercalators [24] whose binding constants have been found to be in the order of 10^6-10^7 M^{-1}.

$$(\varepsilon_a - \varepsilon_f)/(\varepsilon_b - \varepsilon_f) = \left[b - (b^2 - 2Kb^2 a\,[DNA]/S\right]^{1/2}/2\,KbC_t$$
$$B = 1 + KbC_t + Kb\,[DNA]_t/2S$$

Where ε_a is the extinction coefficient absorbed for the charge-transfer absorption band at a given DNA concentration, ε_f is the extinction coefficient of the complex free in solution.

ε_b is the extinction coefficient of the complex when fully bound to DNA. Kb is the equilibrium binding constant, C_t is the total metal complex concentration, [DNA] is the DNA concentration in nucleotides, and S is the binding site size in base pairs [25].

Generally, intercalators show bathochromic shift and hypochromism. In the present work, with the addition of DNA, hyperchromism accompanied by moderate red shift of 3 nm in the absorbtivity of inter ligand bands are observed. Such a small change in λ_{max} is more in keeping with external binding, leading to small perturbations.

3.7.2. Fluorescence studies

The fluorescence titration is used to characterize the interaction of complexes with DNA following the changes in fluorescence intensity of the complexes. The interactions between the complexes and DNA can prevent the fluorescence emission of the complexes from being quenched by polar solvent molecules and result in the enhancement of fluorescence intensity [26].

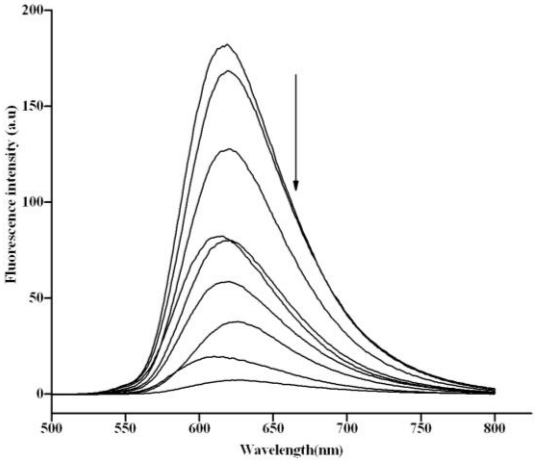

Fig. 6. The emission spectra of the DNA-EB system with increasing amounts of Ru(II) and Pd(II) complexes.

Steady-state emission quenching experiments are used to observe the binding mode of the compounds to DNA. EB (ethidium bromide) can intercalate nonspecifically into DNA, which causes it to fluoresce strongly. Figure 6 & 7 shows the emission spectra of the DNA-EB system with increasing amounts of Ru(II) and Pd(II) complexes. The emission intensity of DNA-EB system decreases as the concentration of the complexes increases, which indicates that the compound could displace EB from the system. The quenching plots illustrate that the quenching of EB bound to DNA by the compounds are in good agreement with the linear Stern-Volmer equation. The Kq values for the Pd(II) and Ru(II) complexes are 9.1×10^4 and 3.1×10^5 M^{-1}. The data show that the interaction of the Ru(II) complex with DNA is stronger than Pd(II) complex which is consistent with the observed fluorescence spectra.

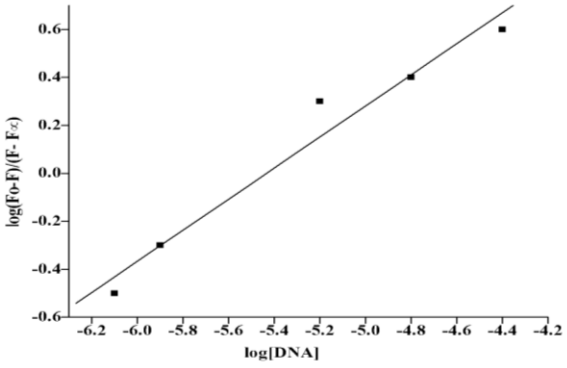

Fig.7. The emission spectra of the DNA-EB system with increasing amounts of Ru(II) and Pd(II) complexes.

3.7.3. DNA cleavage of Ru(II) complexes

The potential to cleave the DNA by the present complexes is studied by gel electrophoresis using super coiled pUC19 DNA in Tris buffer (pH 7.1) and the gels are analyzed after ethidium bromide staining. The mechanistic aspects of the DNA cleavage involving $(bhct)_2Pd$ and $(bhct)_2Ru$ complexes (Fig. 8) shows the gel electrophoretic separation of pUC19 DNA induced by an increasing amount of complexes in the presence of ascarbate. The results in Fig.8. indicate that form I plasmid DNA is gradually converted into form II counterparts with the addition of Ru(II) complex (lane 7-8 in Fig.8) . Further, increase in the amount of 35 µM causes a complete transformation of plasmid DNA from form I to Form II. These phenomena imply that $(bhct)_2Ru$ complexes induces the cleavage of pUC19 DNA intensively in the presence of ascorbate.

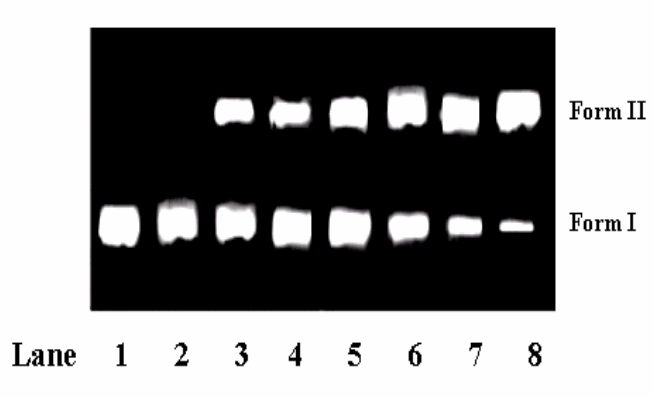

Fig.8. The DNA cleavage involving $(bhct)_2Pd$ and $(bhct)_2Ru$ complexes

3.7.4. Cytotoxic effects of Ru(II) complexes

The MTT cell proliferation assay is a reliable way to measure the cell proliferation rate, and conversely when metabolic events lead to apoptosis or necrosis [27]. The anti-proliferative properties of chemical compounds are evaluated by colorimetric method using ELISA reader while the apoptogenic effects are determined through observing typical fluorescence morphological changes of apoptosis. The data obtained by the MTT assay show that all the complexes have inhibitory effects on the growth of MCF-7 human breast cancer cells in dose-dependent manner (Fig.9).

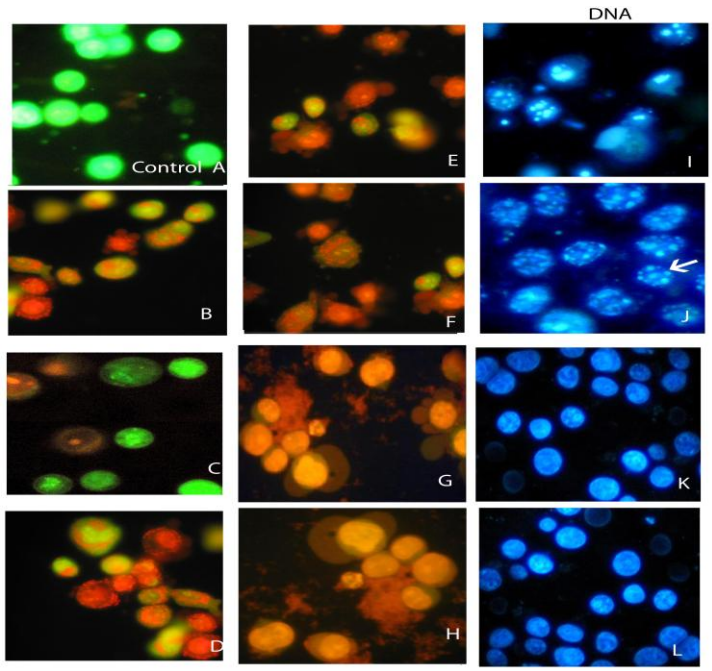

Fig. 9. anti-proliferative properties against MCF-7 cells

The result of current study reveals that maximal number of synthetic compounds possess promising anti-proliferative properties against MCF-7 cells. However, most of the compounds exhibit lowest IC_{50} concentrations obtained towards human breast cancer cells (MCF-7). Therefore, all investigations regarding the apoptogenic property of synthetic compounds were carried on MCF-7 cell line. The inhibitory effect of $(bhct)_2Pd$ on cultured MCF-7 cells are most appreciable because it can produce high frequency of cytotoxicity. The $(bhct)_2Ru$ chemical compound also has greater potential against MCF-7 cells by exposing cells and similar range of concentration of compound required to kill the cells ranging from 42-55 µM/ml. Prominent necrosis and prominent apoptosis are also produced. This sensitivity of tumor cells is quite significant for the chemopreventive action of $((bhct)_2Ru$ of the particular compound.

The good anticancer activities of the Pd(II) and to a lesser extent of Ru(II) complexes against these cell lines is attributed to their planar structure which is documented to avoid possible steric hindrance during physiological actions [28]. Thus, coordination enhances anticancer activities of MCF-7 cells [29], with the exception of the Mn(II) complex which is inactive like the ligand.

4. Conclusion

The newly synthesized organic compound acts as bidetate ligand. The metal ion is coordinated through the amide nitrogen and thionyl sulfur atoms. The bonding of ligand to metal ion is confirmed by the analytical, spectral and magnetic studies. The DNA binding and cleavage properties of synthetic metal complexes are comprehensively studied by different methods including electronic absorption spectra, emission spectra and agarose gel electrophoretic studies. As evident from the cytotoxicity data, the Pd(II) complex proves to be the most potent cytotoxic agents towards breast cancer cell line MCF-7, which implies that the presence of both thiosemicarbazone and metal ion is an important prerequisite for optimal activity for these compounds.

5. Acknowledgement

This research has been supported by UGC for financial assistance of RGNF (Rajiv Gandhi National Fellowship). We thank to Madurai Kamaraj University for providing research and technical facilities.

References

1. **Sahoo, B.K., Ghosh, K.S. Bera, R. and Dasgupta S. (2008).** Studies on the interaction of diacetylcurcumin with calf thymus-DNA. Chem. Phys. Vol. 351 pp 163-169.

2. **Mark R. Waterland, Timothy J. Simpson, Keith C. Gordon and Anthony K. Burrell.(1998).** Spectroelectrochemical studies and excited-state resonance-Raman spectroscopy of some mononuclear rhenium(I) polypyridyl bridging ligand complexes. Crystal structure determinationof tricarbonylchloro [2,3-di(2- pyridyl)quinoxaline]rhenium(I). Dalton Transactions 185-192.

3. **Qi GF, Yang ZY, Qin DD.(2009).** Synthesis, characterization and DNA-binding properties of the Cu(II) complex with 7-methoxychromone-3-carbaldehyde-benzoylhydrazone. Chem Pharm Bull (Tokyo). Vol. 57(1) pp 69-73.

4. **Yan An, Yan-Yong Lin, Hui Wang, Hong-Zhe Sun, Ming-Liang Tong, Liang-Nian Ji and Zong-Wan Mao**. **(2007).** Cleavage of double-strand DNA by zinc complexes of dicationic 2,2′-dipyridyl derivatives. Dalton Trans.**,** pp 1250-1254.

5. **Katritzky A.R., Wang Z, Marson C.M, Offerman R.J., Koziol A.E., Palenik G.J. (1990).** 'Vilsmeier Reactions of 2-Alkyl-2-cyclohexen-1-ones: a Novel Route to Dihydrobenzaldehydes, the Formation of Allyl Alcohols as By-products, and the X-ray Crystallographic Structure of 3-Chloro-2-methyl-2-cyclohexen-1-ol'. J.Heterocyclic. Chem. Vol. 27 pp 139-145.

6. **Fairlie D.P, Ilan Y, Taube H.(1997).** Oxygen versus Nitrogen Bonding of Carboxamides to Pentaammineruthenium(II/III). Inorg Chem. Vol. 12 pp 1029-1037.

7. **Acharyya R, Dutta S, Basuli F, Peng S.M, Lee G.H, Falvello L.R, Bhattacharya S. (2006).** Rhodium assisted C-H activation of benzaldehyde thiosemicarbazones and their oxidation via activation of molecular oxygen. Inorg Chem. Vol. 6 pp 1252-1259.

8. **Mosmann T, Immunol J,(1983).** Rapid colorimetric assay for cellular growth and survival: application to proliferation and cytotoxicity assays. Methods. Vol. 16 pp 55-63.

9. **K. Harms, S.Wocadlo (1995).** *XCAD-4.* University of Marburg, Germany.

10. **Mosmann T. (1983).** Rapid colorimetric assay for cellular growth and survival: application to proliferation and cytotoxicity assays. J. Immunol. Methods. Vol. 65 pp 55-63.

11.**Omar H. Al-Obaidi, (2012).** Synthesis, Spectroscopic and Antimicrobial Studies of Thiosimecarbazone and Its Co(II), Cu(II) Complexes and the DNA Interactions Studies on Cu(II) Complex. In. Jou.of Modern Chemistry,Vol. 2(3) pp 117-126.

12. **Monica Baldini, Marisa Belicchi-Ferrari, Franco Bisceglie, Pier Paolo Dall Aglio, Giorgio Pelosi, Silvana Pinelli, Pieralberto Tarasconi,(2004).** Copper(II) complexes with substituted thiosemicarbazones of α-ketoglutaric acid: Synthesis, X-ray structures, DNA binding studies, and nuclease and biological activity. Inorg.Chem. Vol. 43 pp 7170- 7179.

13. **Mojtahedi M.M , Saidi M.R , Bolourtchian M , (1999).** novel method for the synthesis of disubstituted ureas and thioureas under microwave irradiation. J. Chem. Res.(S) Vol 12 pp 710-711.

14. **Sonia B, Jimenez P, Fatima M, Linares O, Miguel N, Moreno C, Miguel Q.O,(2008).** Versatile Coordinative Abilities of a New Hybrid Pteridine−Thiosemicarbazone Ligand: Crystal Structure, Spectroscopic Characterization, and Luminescent Properties. Inorg. Chem. Vol. 47 pp 1096-1106.

15. **Lobana T.S, Khanna S, Butcher R.J, Hunter A.D, Zeller M, (2006).** Synthesis, crystal structures and multinuclear NMR spectroscopy of copper(I) complexes with benzophenone thiosemicarbazone, Polyhedron, Vol. 25 pp 2755–2763

16. **Refat M. S, I. M. El-Deen, Z. M. Anwer, S. El-Ghol,(2009).** Bivalent transition metal complexes of coumarin-3-ylthiosemicarbazone derivatives: Spectroscopic, antibacterial activity and thermogravimetric studies. J. Mol. Struct.Vol 920 pp 149-162.

17. **Bao-dui-Wang, Z. Yin Yang, D. Dong Qin, Z. Ning Chen, (2008).**Synthesis, characterization, cytotoxic activity and DNA-binding properties of the Ln(III) complexes with ethylenediiminobi(6-hydroxychromone-3-carbaldehyde)Schiff-base. J. Photochem. Photobiol. A. Vol. 194 pp 49-58.

18. **S. Dutta, P. K. Bhattacharya, Edward. R. T. Tiekink, (2001).** Synthesis, Structure andRedox Properties of Mixed Ligand Complexes of Trivalent Ruthenium with Deprotonated 2-Carbamoylpyridine Derivatives and 2,2′-Bipyridine. Polyhedron. Vol. 20 pp 2027-2032.

19. **Kar S, Millar T.A, Chakraborty S, Sarkar B, Pradhan B, Singh R.K, Kunda T, Ward M.D, Lahiri G.K,(2003).** Synthesis, mixed valence aspects and non-linear optical properties of the triruthenium complexes $[(bpy)_2RuII)_3(L)]^{3+}$ and $[(phen)2RuII)_3(L)]^{3+}$(bpy = 2,2′-bipyridine, phen = 1,10-phenanthroline and L^{3-}= 1,3,5-triazine-2,4,6-trithiol). Dalton Trans. pp 2591-2596.

20. **Rebolledo A.P, Vieites M, Gambino D, Piro O.E, Castellano E.E, Zani C.L, Souza-Fagundes E.M, Teixeira L.R, Batista A.A, Beraldo H, (2005).** Palladium(II) complexes of 2-benzoylpyridine-derived thiosemicarbazones: spectral characterization, structural studies and cytotoxic activity. J. Inorg. Biochem. Vol. 99 pp 698–706.

21. **Kovala-Demertzi D, Domopoulou A, Demervzis M.A, Valle G, Papageorgiou A.(1997).** Crystal structure of chloro(2-acetylpyridine N(4)-ethylthiosemicarbazonato) palladium(II). Synthesis, spectral studies, *in vitro* and *in vivo* antitumour activity. J. Inorg. Biochem. Vol. 68 pp 147–155.

22. **Diaz A, Cao R, Fragoso A, Sanchez I, (1999).** Interpretation of the SOD-like activity of a series of copper(II) complexes with thiosemicarbazones. Inorg.Chem. vol. 2 pp 358-360.

23. **Papathanasis L, Demertzis M.A, Yadav P.N, Kovala-Demertzi D, Prentjas C, Castineiras A, Skoulika S, West D. X. (2004).** Palladium-(II) and platinum(II) complexes of 2-hydroxy acetophenone N (4)-ethylthiosemicarbazone -crystal structure and description of bonding properties. Inorg. Chim. Acta Vol. 357 pp 4113-4120.

24. **Wolf A, Shimer A.G, Meehan T, (1987).** Polycyclic aromatic hydrocarbons physically intercalate into duplex regions of denatured DNA. Biochemistry. 26. pp 6392-6396.

25. **Senthilraja D, Bhuanesh N.S.P, Natarajan K, (2012).** Synthesis, crystal structure and pharmacological evaluation of two new Cu(II) complexes of 2-oxo-1,2-dihydroquinoline-3-carbaldehyde (benzoyl) hydrazone: a comparative investigation. Eur. J. Med. Chem. Vol. 47 pp 73-85.

26. **Yu-Lan Song, Yan-Tuan Li, Zhi-Yong-Wu, (2008).** Synthesis, crystal structures and DNA-binding properties of two new mononuclear copper(II) complexes. Trans. Met. Chem. Vol. 33 pp 781-789.

27. **Zheng L.W, Wub L.L, Zhao B.X, DongW.L, Miao J.Y , (2009).** Synthesis of novel substituted pyrazole-5-carbohydrazide hydrazone derivatives and discovery of a potent apoptosis inducer in A549 lung cancer cells. Bioorg. Med. Chem. 17 pp 1957-1962.

28. **Bolos C.A, Nikolov G.S.T, Ekateriniadour L, Kortsaris A, Kyriakidis D.A,(1998).** Structure-Activity Relationships for Some Diamine, Triamine and Schiff Base Derivatives and their Copper(II) Complexes. Metal Based Drugs. Vol. 5 pp 323-332.

29. **Aderoju Amoke Osowole,(2012).** Synthesis, physicochemical and in-vitro antibacterial properties of some novel,metal(II)complexes of 3-([(6-methoxypyridin-3-yl)imino]methyl)naphthalen-2-ol, Elixir Appl. Chem. Vol. 48 pp 9325-9328